



# Experimental study and mathematical modelling of face milling forces of high-strength high-viscosity shipbuilding steel

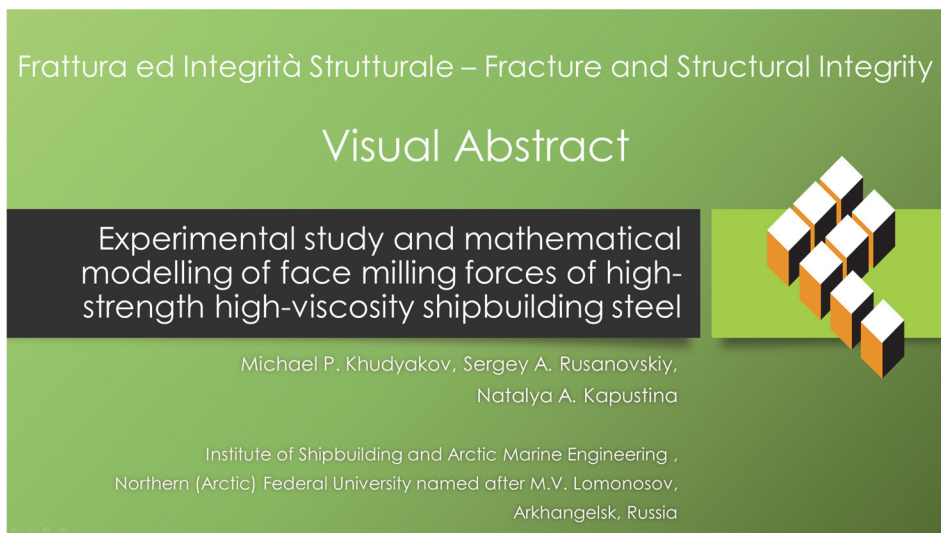
Michael P. Khudyakov, Sergey A. Rusanovskiy, Natalya A. Kapustina

*Northern (Arctic) Federal University named after M.V. Lomonosov, Russia*

*m.khudyakov@narfu.ru, <https://orcid.org/0000-0001-7008-6039>*

*s.rusanovskiy@narfu.ru, <http://orcid.org/0009-0005-6092-1906>*

*kapustina.n@edu.narfu.ru, <http://orcid.org/0000-0002-9770-771X>*



**Citation:** Khudyakov, M.P., Rusanovskiy, S.A., Kapustina, N.A., Experimental study and mathematical modelling of face milling forces of high-strength high-viscosity shipbuilding steel, *Frattura ed Integrità Strutturale*, 69 (2024) 129-141.

**Received:** 20.03.2024

**Accepted:** 19.04.2024

**Published:** 27.04.2024

**Issue:** 07.2024

**Copyright:** © 2024 This is an open access article under the terms of the CC-BY 4.0, which permits unrestricted use, distribution, and reproduction in any medium, provided the original author and source are credited.

**KEYWORDS.** Non-stationary technological complex, Face milling, Bevel faces, Ship hull structure, High-strength high-viscosity shipbuilding steel.

## INTRODUCTION

An important process of assembly and welding in shipbuilding is preparing the edges of holes for the installation of hull saturation parts [1]. The edges of holes in the thick-walled hull structures where these parts are installed must be beveled to perform welding [2]. The cross-sectional shapes of the edge bevels for welded joints are standardized and determined based on the thickness of the parts, the material properties, and the type of a welded joint [3].

As a result of the bevel surface treatment, the edges of the welded joint acquire a complex geometric shape and position in space. This is caused by the type of cutting tool used, the structural curvature of the hull, and the orientation of the saturation part relative to the axes of the hull structure. To describe the complex spatial geometric shape of the edges of

hull structures for welding, the cross-sectional method is used. The specific features of forming the edges of holes for welding of hull structures with single and double curvatures as well as some related issues are discussed in [4].

Increased efficiency of machining of spatially complex surfaces can be accomplished through automation. That is why the machining of such surfaces is performed on stationary multi-axis automated machines whenever possible, at the pre-slipping assembly of a ship's hull. However, a significant amount of such works must be performed directly on the slipway with a fully assembled ship's hull. Relatively simple surfaces in terms of location and configuration, can be machined using non-stationary machines with manual control. However, mechanical machining of the surfaces with more complex shape formations in slipway conditions requires the use of non-stationary equipment with numerical control on three to five axes simultaneously. Non-stationary technological complexes (NTC) with numerical control (NC) are used for the mechanical processing of conoidal hole surfaces in the large-sized hull structures with single and double curvatures. As a rule, NTC have reduced rigidity and vibration resistance compared to stationary equipment [5, 6]. Providing effective application of NTC at machining of ship hull structures in slipway conditions is an important design and technological task.

The main factors restraining the automation of the process are lack of a formalized mathematical representation of the complex spatial shape of welded joint edges and the difficulty of forming movements during their machining [7]. To address these problems, it is necessary to use multi-axis CNC equipment and a methodology linking the production object and production means into a unified technological system [8, 9].

Non-stationary technological complexes (NTC) (see Fig. 1) for multi-axis machining, including those based on industrial robots, are known to have been used for this task. [10]. NTC enable non-stationary multi-axis machining using an industrial robot equipped with a milling spindle and milling cutter [11].

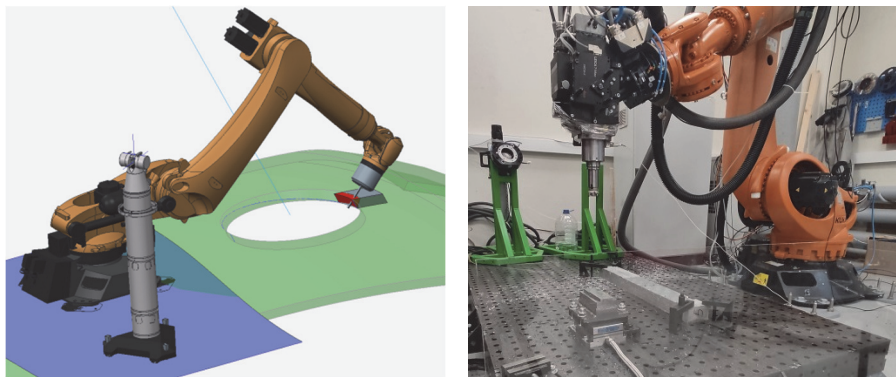


Figure 1: Mechanical processing by means of non-stationary technological complexes.

This type of equipment allows for the machining of complex surfaces and the expansion of the working area through additional controlled axes [12]. However, taking into account the cantilever-jointed design, the maximum permissible load values for robotic NTC are one to two orders of magnitude lower than for corresponding stationary machines with sliding or rolling guides [13, 14]. In this case, usually a configuration of the robot manipulator for face milling which provides the greatest rigidity along the spindle axis is chosen. At the same time, great cutter vibrations in these robotic NTCs occur in the cutting plane [15-17]. Intensive vibrations may occur during robotic milling of difficult-to-machine shipbuilding steels with special viscous and strength properties. These vibrations negatively affect the stability of the machining process and the quality of the machined surface [18]. Thus, when milling steel hull structures in slipway conditions, industrial robots may not have sufficiently rigid, accurate and vibration resistant. This problem can to a certain extent be solved by using adaptive robotic technological complexes [19-22]. Adaptability is ensured by the presence of feedback between the executive link and the control unit. To increase rigidity and vibration resistance of the machine structure and to ensure the required machining accuracy, a promising solution is the use of non-stationary technological complexes with CNC (computer numerical control) with parallel kinematics [23].

To address the need of automating the processing of hull structures in slipway conditions, the authors have developed a methodology for designing non-stationary technological complexes. This methodology is based on a unified mathematical model for describing the production object, process, and means of production [24]. Within this methodology, NTC is considered as a complex system in which each functional component is represented by a local subsystem connected to other subsystems by direct and feedback links.



The work [25] presents a mathematical matrix model that combines a description of the production object and individual components of the NTC. Decomposition of the blocks intended for forming the edges of holes of the hull structure and the theoretical determination of loads on the cutter are carried out.

The main aim of this article is to develop a mathematical model of the milling forces acting on the edge surface of the hull structure. The results presented in the article are an important stage in the implementation of the methodology proposed in [25]. The experimental model that has been developed is the starting point for designing modules of cutting tools, equipment, and tooling in accordance with the NTC design methodology. The Data obtained through the modeling will be fed to the input of the next stage of the NTC's design, ensuring stiffness and deformation accuracy.

The article discusses a promising type of machining for automated non-stationary machining of edges of holes of hull structures – high-speed face milling. This type of milling reduces the value and variation of the components of the cutting force acting on the cutting tool and the NTC as a whole.

There is a substantial body of literature that discusses creating mathematical and simulation models of milling processes [26]. The issues of increasing vibration resistance of mobile equipment with low rigidity have been also highlighted in many studies. The authors note that milling with non-stationary equipment is the most complex and poorly researched process. This complexity is explained by the presence of several cutting edges, variable allowances, discontinuity and impact nature of the milling process.

As has been noted in a number of studies [27-29], the initial data for creating a milling model is the geometric model of the surface being processed, the initial geometric characteristics of the cutting tool, the viscosity-strength characteristics of the material, and the trajectory of the tool. Through the matrix representation of the complex model [24], the cutting force model is easy to transform and embed into the general NTC design methodology. As the results of preliminary tests have shown, to simulate the cutting process, a planar milling scheme can be used.

Due to the main aim of the article, which is to identify the mathematical dependence between the cutting forces and the main technological characteristics of the cutting process: feed rate, cutting speed, cutting depth, – a factorial experiment of face milling of a workpiece from material used for the production of ship hull structure was planned and carried out. The depth of cut  $t$ , the speed of the main movement (cutting)  $V$ , and the speed of the forming movement (feed rate)  $s$  were determined as influencing factors.

High-performance processing of high-strength steel can be difficult due to the special chemical, mechanical and thermophysical properties of the material. When processing high-strength steels, increased wear and, consequently, instability and low efficiency of the cutting process can be observed. As the authors of [30] have demonstrated, the cutting force is mostly influenced by the feed to the tooth and the cutting depth. The cutting force (from the influence of the feed rate and the depth) and temperature (from the influence of the cutting speed) have, in turn, the greatest influence on the tool wear. Additionally, as has been shown in [31], the cutting speed has the greatest effect on reducing the cutting force. When the red hardness limit of the processed material is reached, its hardness decreases and, as a result, the cutting forces decrease. Therefore, the method of speed milling of a workpiece made of high-strength steel was chosen for the experiment.

The mathematical model was developed on the basis of experimental data in the field of mechanical processing of ship hull alloys with specific viscosity and strength properties. Due to the lack of statistical data, it is difficult to create a stable analytical model for calculating cutting forces. Cutting materials and tool designs are constantly evolving, making it necessary to investigate the cutting process in a laboratory setting and create an empirical model.

Additionally, as a theoretical study of this issue has revealed, the field of high-speed cutting of high-strength materials has not been thoroughly explored, necessitating the use of empirical data. Several authors have proposed approaches to the analytical definition of cutting forces. However, these approaches have not yet been incorporated into the current engineering methodology, as they contain inaccuracies when it comes to determining the friction forces on the cutting wedge surfaces and the distribution of normal and tangential stresses. The clarification of these data can only be achieved through experimental studies of cutting processes.

## METHODS AND MATERIALS

### *Explanation of research methods*

The experimental method of measuring cutting forces and creating empirical formulas is essential to understanding the cutting process of materials. This method has been used since the beginning of scientific research in this area. The collection of data and creation of empirical models have become the basis for reference books and practical guides for designers and engineers in the field of material processing.

An extensive range of analytical and numerical models have been developed for modeling of the cutting process [32]. The models used for finite element analysis (FEA) are currently considered to be the most universal.

The finite element method is widely used to predict the cutting characteristics of metals, such as tool wear and plastic deformation of the workpiece. FEA is based on various fracture models. Among there, we can mention the models based on damage accumulation mechanics, such as the Cockroft-Latham model [32], the Wilkins model [32] and the Johnson-Cook [32] fracture model. The most popular Johnson-Cook fracture model expresses the effect of triaxial stress, strain rate and temperature on the strain to fracture. In this model, fracture constants relative to different effective factors are usually calibrated separately. However, when using the Johnson-Cook fracture model we often encounter a problem of acquiring and calibrating fracture constants for the specific material.

For the tested material, we were unable to obtain fracture constants that adequately describe the process over the entire range of cutting modes under study. For this reason, we decided to first develop a regression model. This model aims to identify the characteristic ranges and causes of rapid changes in cutting forces with sudden changes in the influencing factors.

This article aims to address the challenge of developing an empirical model for high-speed cutting of shipboard steel in order to integrate it into the algorithm for constructing special equipment - NTC - for processing hull structures under non-stationary conditions. While a more in-depth examination of the high-speed milling process is beyond the scope of this work, we hope that the findings may contribute to a better understanding of theoretical models for cutting forces in milling.

Data preprocessing is carried out by array processing methods and mathematical statistics methods in the MS Excel software package. The analysis includes highlighting the area of steady cutting on the graph of the cutting forces, where the required number of points for processing is determined. Based on the resulting array of points, a graph of oscillations of the cutting forces components (see Fig. 2) is obtained; the peaks of values for one cutting insert, which increase with the dynamic effect, are defined. The average value of the cutting force component  $F_{xy}$  is calculated of the peak cutting forces as they can cause the overloading of the NTC mechanism.

The radial  $F_r$  and tangential  $F_t$  components of the cutting force are determined for each experiment based on a geometric analysis of the milling scheme and taking into account the milling direction (see Fig. 2). Finally, the models of the milling forces are obtained using regression analysis performed in the MS Excel analysis package.

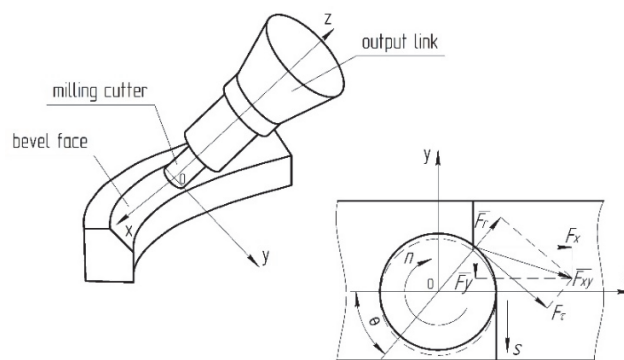


Figure 2: The scheme for cutting force components in plan in the cut-down milling process.

### *Tool and equipment*

When designing NTCs, it is important to take into account the relatively low rigidity of their supporting structures compared to stationary equipment. From the point of view of stability of the cutting process, the most critical factors are the tangential and radial components of the cutting force. From the point of view of forming accuracy, the most significant factor is the value of the axial component of the cutting force [33]. This is true both for the NTCs of a multilink structure (based on parallel kinematics mechanisms) and, especially, for the NTCs of a single-link structure.

With the above in mind, an F90-LNHU13R-D50Z6S22 end mill with a diameter of 50 mm was used (see Fig. 3, a). In order to reduce all the three components of the cutting force, the cutter was equipped with the inserts LNHU130608R-YG602 from YG-1 (see Fig. 3, c) with positive radial and axial front angles. The WKP25S alloy with Tiger•tec® Silver CVD coating is recommended by the manufacturer when machining high-strength steels. The right-hand insert has a countersunk hole for tangential mounting in the cutter body by means of a screw. The thickness of the insert is  $6.35 \pm 0.025$  mm; the cutting edge length is 13 mm. The rounding radius of the cutting edge is 0.8 mm. It is intended for

semi-finishing and finishing machining. The insert is rectangular in plan and has zero radial, axial and peripheral relief angles. The radial and axial rake angles are set structurally positive and equal to 13 degrees each. The peripheral relief angle is given by its position in the cutter body seat and is 8 degrees. The peripheral clearance angle of chamfer is 3 degrees. The axial rake angle after the insert is installed in the cutter body is 8 degrees. The lead angle is 90 degrees. A CNC milling machine Emco Concept Mill 250 was used to process the surface of the workpiece (see Fig. 3, c).



Figure 3: The CNC milling machine Emco Concept Mill 250 and the milling cutter.

A three-component dynamometer M30-3-6K with a computer recorder from Tilcom was used to measure the values of cutting force components in the three directions (see Fig. 4, a).

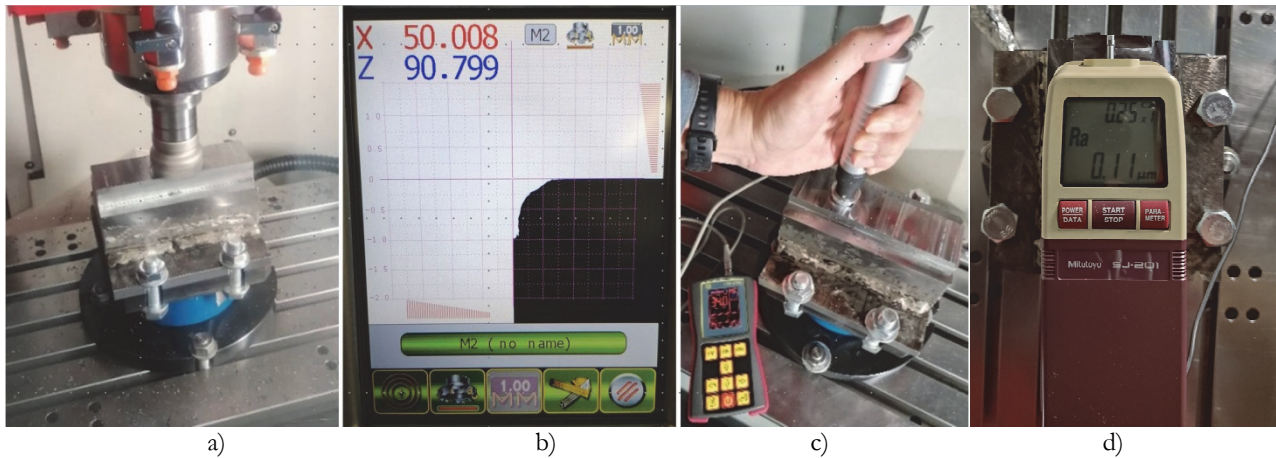


Figure 4: Milling, wear measurement and hardness measurement processes.

In order to reduce the mutual influence of adjacent inserts on the results and to maintain the balance of the cutter, two radially opposed inserts were installed. The pre-processed workpiece was installed with alignment along the axes of the machine. The position of the inserts within the cutting body and their wear were periodically monitored using a Nikken device (see Fig. 4, b).

In general, quality indicators of the machined surface are roughness, hardness, and residual stresses. In the case of bevel faces for a welded joint, surface roughness and hardness after machining are the most significant indicators. These two indicators were measured using a portable ultrasonic hardness tester TKM-469 (see Fig. 4, c) and a profilometer Mitutoyo SJ-201, respectively (see Fig. 4, d).

#### *Processed material*

A pre-processed workpiece with a rectangular protrusion with the dimensions of (L×B×H) 70×40×20 mm was milled (see Fig. 4). The steel type AB6A that has the following viscosity-strength characteristics: tensile strength is more than 900 MPa, KCU is more than 65 J/cm<sup>2</sup>, HRC 34, – was used to produce the workpiece.



### Milling scheme and operating modes

An asymmetric milling scheme was implemented in the experiment (see Fig. 2). According to the plan of the experiment, the depth of cut  $t$  varies from 0.5 mm to 2 mm, feed rate  $s$  varies from 0.02 to 0.1 mm/tooth, cutting speed  $V$  varies from 180 m/min to 280 m/min. The Processed surface had the length of 40 mm in each pass. Working passes are carried out in both directions to implement cut-up and cut-down milling. The milling width was 8 mm in each working pass. The cutting modes were set and monitored during machining using the machine's CNC control panel. The machine has a built-in monitoring system for extreme vibrations and drive power, which ensured that experiments were carried out under normal operating conditions of the machine.

When machining bevel faces for welding in the holes on cylindrical, conical, spherical and similar surfaces of body structures, the allowance to be removed is not uniform. Accordingly, the conditions of stock removal and cutting forces are variable. Therefore, in the experiment, cutting forces were measured over the entire cutting section, including the plunge and exit areas of the cutter from the material. The steady-state cutting section during the processing of the results was used to determine the average values of the cutting force in order to create a mathematical model of the face milling process. The discrete step time of measurements using dynamometer M30-3-6 K with a computer recorder from Tilcom was 0.0004 s.

Coolant was not used during the milling process.

In addition to the measurements of quantitative parameters, visual qualitative control of the wear character of the cutting edge of the inserts, as well as the shape and appearance of the chips that were formed, was performed. This is important from the point of view of both the quality of the cutting process and the safety of machining in an operating production facility.

## RESULTS

During the experiment, the instantaneous values of cutting force components were recorded with a discrete step of 0.0004 s, as has been mentioned above. A total of 54 experiments were conducted for three variable factors  $t, s, V$  and the three levels of their values, twice for cut-up and cut-down milling. Data processing was carried out in the order described in the previous section. The values of the variable factors are presented in Tab. 1.

$t$ , mm	$s$ , mm/tooth	$V$ , m/min
0.5	0.02	180
1.5	0.06	230
2	0.1	280

Table 1: The values of the variable factors.

Let us now take a closer look at the data analysis process, using the results from one experiment as an example. The graph of the oscillations of the cutting forces components under the following operating modes is constructed (see Fig. 5): cutting direction is cut-down milling,  $t = 1.5$  mm,  $s = 0.1$  mm/tooth,  $V = 180$  m/min.

The steady-state cutting area is highlighted after the initial data analysis according to the graph in Fig. 5 and is represented by a separate array.

A graph of the oscillations of the cutting force component  $F_{xy}$  during cut-down milling is shown in Fig. 6.

A similar representation is a graph of the oscillations of the cutting force component  $F_{xy}$  during cut-up milling – see Fig. 7. The values of  $F_{xy}$  cutting force component are calculated for the peaks of  $F_x$  and  $F_y$  components during cut-up milling.

The graph of the  $F_{xy}$  rate is shown in Fig. 8, the cutting time is 2.7751 s, and the length of cutting is 10.6 mm. The choice of the components for determining the peaks is due to the special distribution of the forces for each of the milling directions based on the milling scheme – see Fig. 2. The maximum of allowance is cut off in the first moments of cutting by one insert in cut-down milling and  $F_x$  reaches the maximum value, whereas in cut-up milling, the maximum of allowance falls at the end of cutting, where  $F_y$  takes maximum values – see Fig. 6, 7.

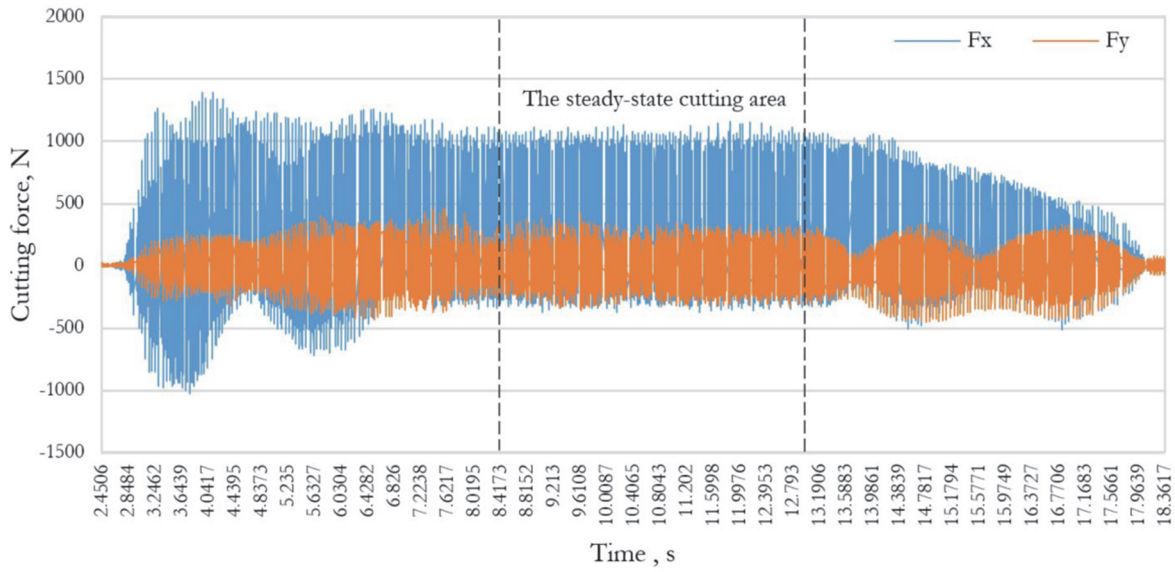


Figure 5: Cutting forces rate in the cut-down milling process ( $t = 1.5$  mm,  $s = 0.1$  mm/tooth,  $V = 180$  m/min).

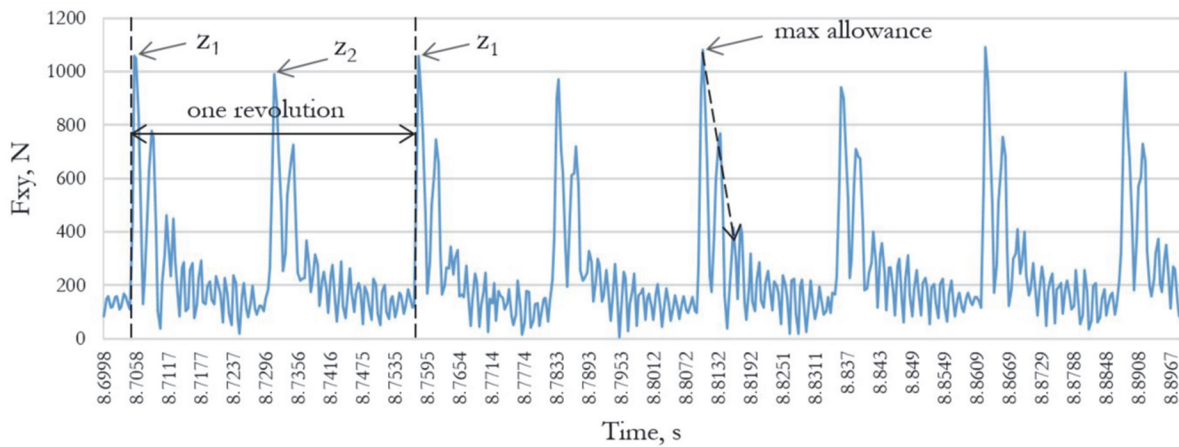


Figure 6: The amplitude curve of  $F_{xy}$  in the cut-down milling process ( $t = 1.5$  mm,  $s = 0.1$  mm/tooth,  $V = 180$  m/min).

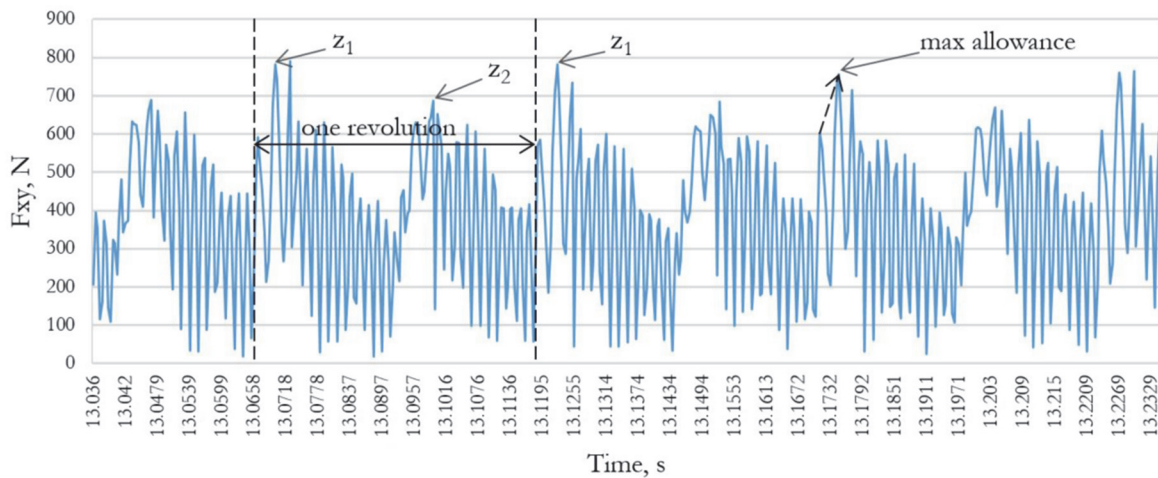


Figure 7: The amplitude curve of  $F_{xy}$  in the cut-up milling process ( $t = 1.5$  mm,  $s = 0.1$  mm/tooth,  $V = 180$  m/min).

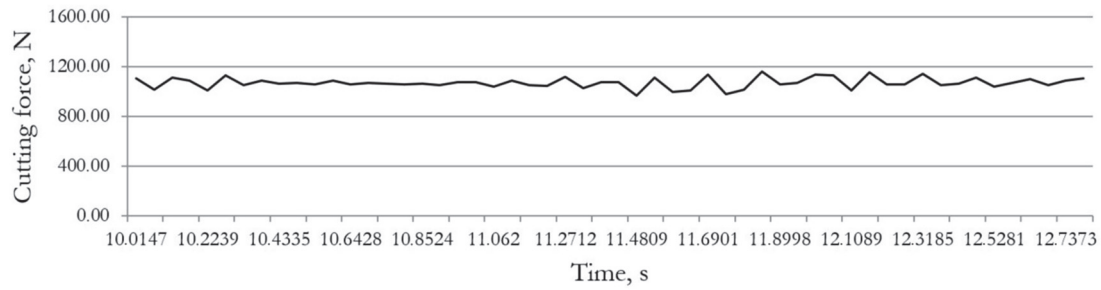


Figure 8:  $F_y$  maximum rate in the cut-down milling process ( $t = 1.5$  mm,  $s = 0.1$  mm/tooth,  $V = 180$  m/min).

After analyzing the resulting data set, the following mathematical models for the milling force components,  $F_r$  and  $F_\tau$ , were obtained:

– in the cut-up milling process

$$F_r^u = 191.246t^{0.822} s_\tau^{0.359} V^{-0.245}, \quad (1)$$

$$F_\tau^u = 19.532t^{0.732} s_\tau^{0.277} V^{-0.710}, \quad (2)$$

– in the cut-down milling process

$$F_r^d = 15776.5t^{0.929} s_\tau^{0.323} V^{-0.543}, \quad (3)$$

$$F_\tau^d = 17775.839t^{0.753} s_\tau^{0.627} V^{-0.365}. \quad (4)$$

The force amplitude over time for each component of the cutting force is shown in Fig. 9.

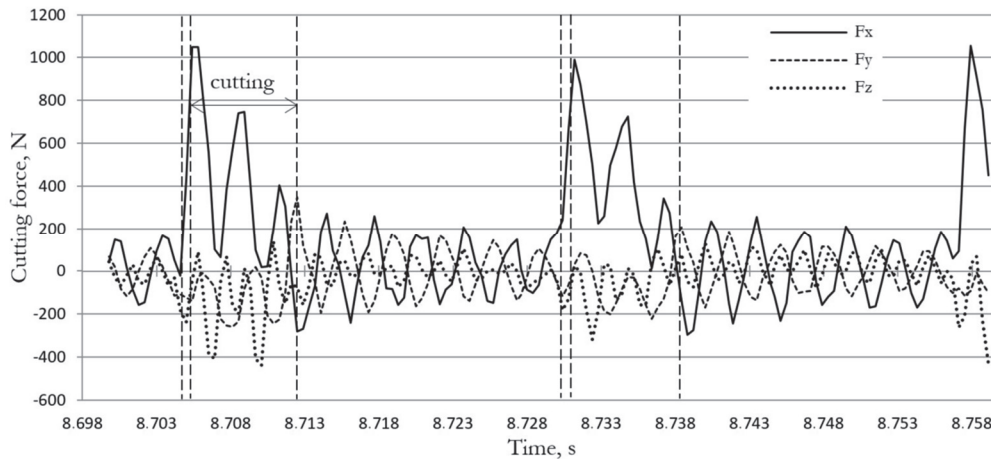


Figure 9: The force amplitude curves in the cut-down milling process ( $t = 1,5$  mm,  $s = 0,1$  mm/tooth,  $V = 180$  m/min).

## DISCUSSION

**A**s a result of the experiment and analysis of the obtained mathematical models, it was revealed that:

- The Analysis of the oscillations of the cutting force components (Fig. 5) for the entire time of the pass allowed defining the steady-state cutting area in all the experiments carried out. As a result of 54 experiments the



maximum magnitude of the cutting force  $F_{xy}$  was found to be 1286 N in cut-down milling at the following operating modes:  $t_{max} = 2$  mm,  $s_{max} = 0.1$  mm,  $V = 230$  m/min, – and 1450 N in cut-up milling at identical modes – see Fig. 10–12. It is worth noting that the peak of the  $F_x$  component was defined at the same modes as the component  $F_y$ . The maximum value of the  $F_x$  component is 587 N in cut-down milling and 556 N in cut-up milling, respectively. This conclusion, which is based on experimental data, is consistent with what has previously been discussed in research literature [31];

- Comparing the obtained values of cutting forces with those proposed in the study [34], for various models of industrial robots we can conclude that the operability of the robotic non-stationary equipment is ensured. At the same time, the expected processing accuracy of steel for hull structures has been achieved with a required value of 1-2 mm. The cutting process is therefore possible under given conditions;
- The  $F_{xy}$  amplitude curve reflects the characteristic peak shapes for the cut-down (Fig. 6) and cut-up (Fig. 7) milling processes. It is obvious that in counter milling, under equal working conditions, the amplitudes of oscillations are larger than in cross milling. This process of cut-up milling is characterized by being more energy consuming;
- It is easy to determine the amplitudes of the forces for each tooth using Fig. 6, 7, 9; the distance between the peaks of one tooth corresponds to the estimated turnaround time. The discrete step turned out to be sufficient for a fairly accurate graphical determination of the cutting time per tooth, the time per revolution, which corresponds to the calculated figures;
- The oscillation amplitudes (see fig. 10) of the cutting force components are shift relative to each other, which is explained by the geometry of the milling scheme. During cut-down milling the axial component of the cutting force component  $F_x$  undergoes a disturbance earlier than the cutting process begins by the value of a discrete time step, which can be explained by the effect of a technological “trace” for the previous cutting step. At this point, the force component  $F_x$  also begins to grow, since the height of the “trace” is insignificant. Further, the tooth penetrates into the workpiece and cuts the largest allowance, which is characterized by a sharp increase in the force component  $F_x$ . The peak of  $F_y$  occurs at the moment of insert exit from the workpiece, with the force vector having the largest projection on the OY axis (see Fig. 2);
- The dependence of the cutting forces on the depth of cut is of the greatest importance, the degree indicator has the greatest absolute value within the investigated limits – see Eqn. (1)–(4), Fig. 10. In some cases, the dependence is close to linear – see Eqn. (3);
- The dependence of the cutting forces on the feed rate and cutting speed is non-linear – see Eqn. (1)–(4), Fig. 10, 11;
- The dependence of the cutting force on the cutting speed within the specified limits has a non-attenuating character for cut-up milling, whereas for cut-down milling it has an attenuating character – see Fig. 10, 12. It has previously been shown [35] that with an increase in the cutting speed of structural steels and titanium alloys up to a speed of 240 m/min, all the components of the cutting force decrease monotonically. Verification of the possibility of further increasing the cutting speed requires an additional series of experiments.

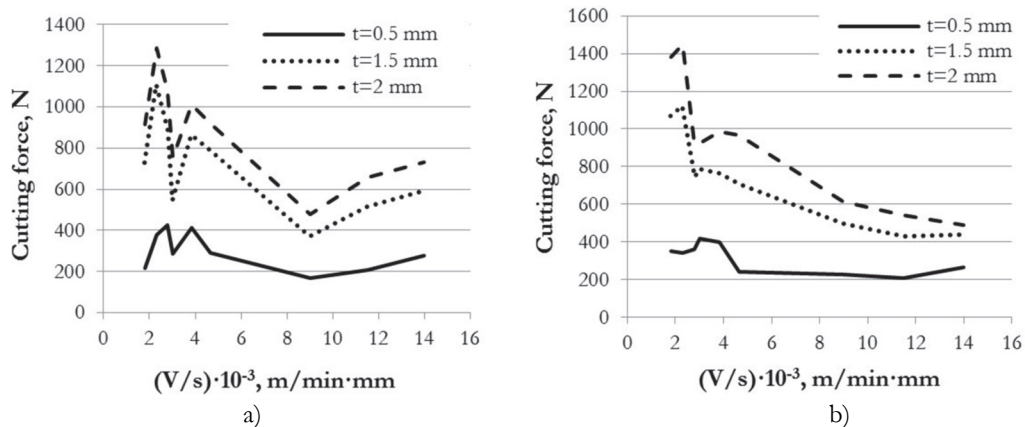


Figure 10:  $F_{xy}$  cutting force component rate under the constant depth of cut: a) in the cut-up, b) in the cut-down milling process.

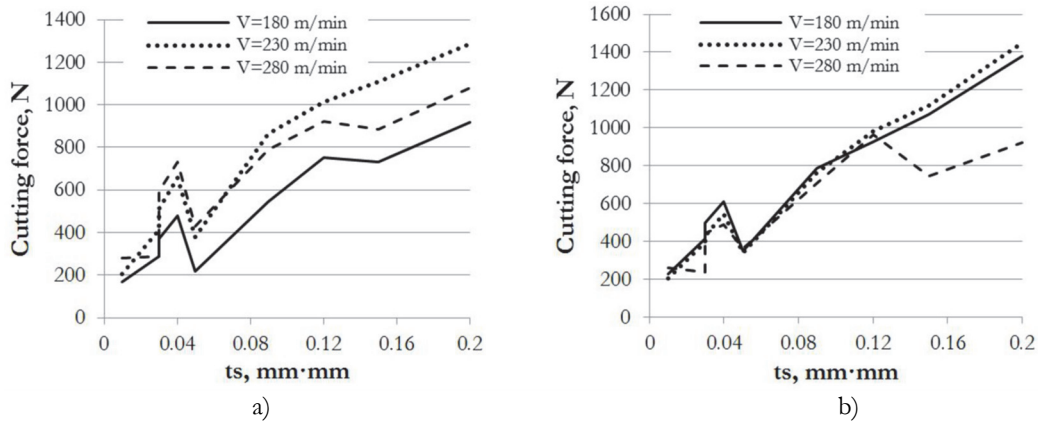


Figure 11:  $F_{xy}$  cutting force rate under the constant cutting speed: a) in the cut-up, b) in the cut-down milling process.

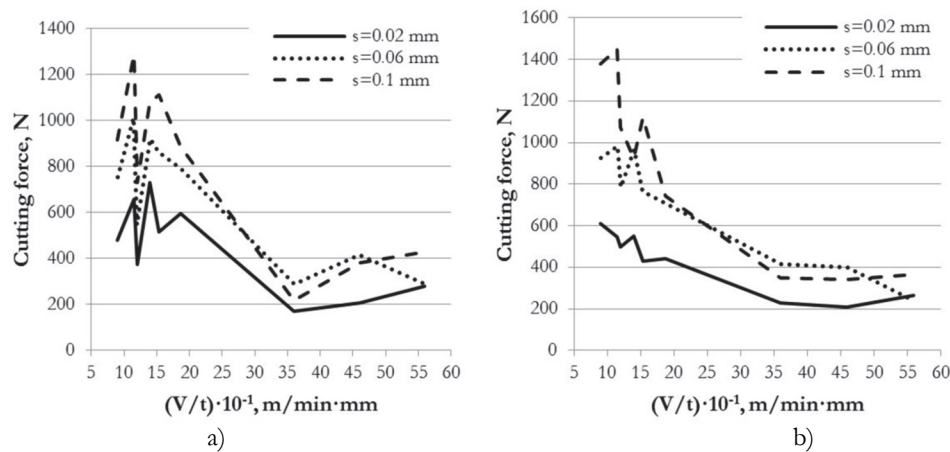


Figure 12:  $F_{xy}$  cutting force rate under the constant cutting feed rate: a) in the cut-up, b) in the cut-down milling process.

## CONCLUSION

The study implemented an experimental method to investigate the milling process of hard-to-process steel, and used mathematical processing of the results. Turning to the main aim of the article, primary result of the study is developing a model of milling forces that occur when beveling edge faces of weld joint in the hull structures. A mathematical description of cutting forces is part of a unified functional model of the object of production, the process, and the means of production. The model of cutting forces which has been transformed into a matrix form is necessary for calculation of instantaneous force inputs to the design modules of tools, equipment, tooling of the general NTC design methodology.

The conducted research has confirmed the possibility and expediency of high-speed milling of parts made of steels with special viscosity and strength properties. The obtained model of face milling forces is currently used to implement the next stage of NTC design - structural and parametric synthesis of the design of a specialized machine tool with parallel kinematics.

The analysis of the oscillation spectrum of experimentally obtained cutting forces showed the absence of dependence between the frequency of the cutting force oscillations at cutting modes and tool geometry.

The obtained experimental results partially confirm the results of other studies [36-39] that the amplitude of the oscillations during cutting is smaller the lower the feed rate and increases with increasing depth of cut. The dependence of the amplitude on the cutting speed has a non-monotonic character.



Additional studies are required to determine the possibility of further increase of machining speed of hard-to-machine shipbuilding steels and alloys. In addition, a wider and more detailed study of the dependence of the magnitude and variability of the cutting force on the cutting speed of these materials in the ranges up to 600...1000 m/min is needed.

The main aim of the article was the computational-experimental development of a mathematical model of forces of hard-to-machine shipbuilding steel face milling. The model obtained based on experimental data allows correcting the theoretical model of cutting, which is a link between the development of cutting tools and the development of equipment and tooling in accordance with the NTC design methodology [40].

The expansion of the cutting force model based on the results of new experiments will make it possible to predict the force response in the machine components with a higher degree of accuracy, to increase the rigidity and vibration resistance of the structure, and respectively, the accuracy and adaptability of machining.

## DECLARATION OF COMPETING INTEREST

The authors declare that they have no known competing financial interests or personal relationships that could have appeared to influence the work reported in this paper.

## ACKNOWLEDGEMENTS

This work was supported by the RSF No. 23-29-10078.

## REFERENCES

- [1] Tsvetkov, Y. N. (2011). *Fundamentals of ship engineering technology*. Federal Agency of Marine and River Transport, Federal State Educational Institution of Higher Professional Education "St. Petersburg State University of Water Communications". Saint-Petersburg. 265 p. ISBN 978-5-88789-331-0.
- [2] Rusanovskiy, S.A., Khudyakov, M.P., Snegireva, K.K. (2021). Study of Shape Forming of Welding Bevel in Openings of Pressure Hulls of Underwater Shipbuilding Objects. In: Radionov, A.A., Gasiyarov, V.R. (eds) *Proceedings of the 6th International Conference on Industrial Engineering (ICIE 2020)*. ICIE 2021. Lecture Notes in Mechanical Engineering. Springer, Cham. DOI: 10.1007/978-3-030-54814-8\_19.
- [3] ASME PVHO-1-2007. (2007). *Safety Standard for Pressure Vessels for Human Occupancy*, edition 2007. The American Society of Mechanical Engineers: New York, America.
- [4] Rusanovskiy, S.A. (2021). *Povyshenie urovnya avtomatizacii mehanicheskoy obrabotki korpusnyh konstrukcij ob'ektov okeanotekhniki v usloviyah stapel'nogo proizvodstva*, PhD Thesis, Severodvinsk.
- [5] Yuchao Du, Zhiqiang Liang, Sichen Chen, Hao Huang. (2023). Dynamic Modeling and Stability Prediction of Robot Milling Considering the Influence of Force-Induced Deformation on Regenerative Effect and Process Damping. *Metals* 13(5):974. DOI: 10.3390/met13050974.
- [6] Xianyang Zhang, Linlin Wan, Xiaoru Ran. (2024). Research progress on the chatter stability in machining systems. *The International Journal of Advanced Manufacturing Technology*. 131(1–4), pp.1-34. DOI:10.1007/s00170-024-13050-8.
- [7] Panagiotis Stavropoulos, Dimitris Manitaras, Harry Bikas, Thanassis Souflas. (2022). Integration of Machining Process Digital Twin in Early Design Stages of a Portable Robotic Machining Cell (In book: *Flexible Automation and Intelligent Manufacturing: The Human-Data-Technology Nexus*). pp. 301-315. DOI:10.1007/978-3-031-18326-3\_30.
- [8] Xinyue Li, Lu Lei, Cheng Fan, Fusheng Liang, Lei Zhang. (2023). Ball-End Cutting Tool Posture Optimization for Robot Surface Milling Considering Different Joint Load. *Applied Sciences*. 13(9). DOI:10.3390/app13095328.
- [9] Xuexin Zhang, Lianyu Zheng, Wei Fan, Wei Ji. (2024). Knowledge graph and function block based Digital Twin modeling for robotic machining of large-scale components. *Robotics and Computer-Integrated Manufacturing*. 85(102609), pp. 1-19 DOI:10.1016/j.rcim.2023.102609.
- [10] IRB 6660 robot. Available at: <https://new.abb.com/products/robotics/robots/articulated-robots/irb-6660>.



- [11] A KUKA milling robot. Available at: <https://www.kuka.com/en-us/products/process-technologies/milling>.
- [12] Milling robotic cell. Available at: <https://www.eurobots.ru/milling-system-en.html>.
- [13] Pandremenos J.t Doukas C., Stavropoulos P., Chryssolouris G. (2011). Machining with robots: a critical review // 7th International Conference on Digital Enterprise Technology. Athens. Greece.
- [14] Fengxia He, yu Liu, Kuo Liu. (2019). A chatter-free path optimization algorithm based on stiffness orientation method for robotic milling. *The International Journal of Advanced Manufacturing Technology*. 101(9–12). DOI:10.1007/s00170-018-3099-y.
- [15] Wenbo Wang, Qiang Guo, Zhibo Yang, Yan Jiang. (2022). A state-of-the-art review on robotic milling of complex parts with high efficiency and precision. *Robotics and Computer-Integrated Manufacturing*. DOI: 10.1016/j.rcim.2022.102436.
- [16] Shihao Xin, Xiaowei Tang, Jiawei Wu, Fangyu Peng, Rong Yan, Wei Yang. (2023). Investigation of the low-frequency chatter in robotic milling. *International Journal of Machine Tools and Manufacture*. 190, 104048. DOI: 10.1016/j.ijmachtools.2023.104048.
- [17] Rusanovskiy, S.A., Khudyakov, M.P., Kovin, P.V. (2024). Modelling technique of the opening's bevel in underwater shipbuilding hulls objects for welding flanges Part 4 Experimental research of the method applicability. *Marine intellectual technologies*. № 1 part 1. pp. 73—80. DOI: 10.37220/MIT.2024.63.1.008.
- [18] Zhongyang Zhang, Juliang Xiao, Haitao Liu, Tian Huang.(2022). Base placement optimization of a mobile hybrid machining robot by stiffness analysis considering reachability and nonsingularity constraints. *Chinese Journal of Aeronautics*. DOI: 10.1016/j.cja.2022.12.014.
- [19] Zhenya He, Hongying Zheng, Haolun Yuan, Xianmin Zhang. (2023). An Orientation Measurement Method for Industrial Robots Based on Laser Tracker. In book: *Intelligent Robotics and Applications*. pp. 273-283. DOI: 10.1007/978-981-99-6504-5\_24.
- [20] Yongzhuo Gao, Haibo Gao, Kunpeng Bai, Mingyang Li, Wei Dong. (2021). A Robotic Milling System Based on 3D Point Cloud. *Machines* 9(12), 355. DOI:10.3390/machines9120355.
- [21] Lihong Zhou, Xiangchao Zhang, Qiangang Zhang, Shaoliang Li, Wanliang Zhao. (2022). Automatic robotic trajectory planning based by laser projection measurement. *Conference: Optical Metrology and Inspection for Industrial Applications IX*. DOI:10.1117/12.2641751.
- [22] Zheng Wang, Runan Zhang, P.s. Keogh. (2020). Real-time laser tracker compensation of robotic drilling and machining. *Journal of Manufacturing and Materials. Processing* 4(3), 79. DOI:10.3390/jmmp4030079.
- [23] Portable Milling Machine - Pentapod PM-Series. Available at: <https://metrom.com/portable-milling-machine/>.
- [24] Rusanovskii, S.A., Khudyakov, M.P., Klimov, Yu.V. (2020). Design of Production Systems. 1. Development of the Design Procedure. *Russian Engineering Research*. 40(10), pp. 815–818. DOI: 10.3103/S1068798X20100226.
- [25] Rusanovskii, S.A., Khudyakov, M.P. (2020). Design of Production Systems. Part 2. Nonstationary Systems. *Russian Engineering Research*. 40 (11), pp. 901–904. DOI: 10.3103/S1068798X20110167.
- [26] Shikang Li, Danian Zhan, Shuoxue Sun, Yuwen Sun. (2023). Dynamics modeling and simultaneous identification of force coefficients for variable pitch bull-nose cutter milling considering process damping and cutter runout. *The International Journal of Advanced Manufacturing Technology*. 130(2), pp.1-22. DOI:10.1007/s00170-023-12777-0
- [27] Yuwen Sun, Yang Liu, Meng Zheng, Jinting Xu. (2023). A review on theories/methods to obtain surface topography and analysis of corresponding affecting factors in the milling process. *The International Journal of Advanced Manufacturing Technology*. 127(2), pp. 1-35. DOI:10.1007/s00170-023-11723-4.
- [28] Chigbogu Ozoegwu, Peter Eberhard. (2023). A literature review on prediction methods for forced responses and associated surface form/location errors in milling. *Journal of Vibration Engineering & Technologies*. DOI: 10.1007/s42417-023-01227-6.
- [29] Jing Ni, Rulan Dai, Xiaopeng Yue, Zheng Junqiang. (2022). Contribution ratio assessment of process parameters on robotic milling performance. *Materials*, 15(10), 3566. DOI:10.3390/ma15103566.
- [30] Cen, L., Melkote, Sh.N. (2017). Effect of robot dynamics on the machining forces in robotic milling. *Procedia Manufacturing*, 10, pp. 486-496. DOI: 10.1016/j.promfg.2017.07.034.
- [31] Mazur, N.P. (2013). *Osnovy teorii rezaniya materialov (Fundamentals of the theory of cutting materials)*, NTU “Kharkiv Polytechnic Institute”, Kharkiv.
- [32] Corina Constantin, Eugen Străjescu. (2011). Revision of actual stage in modeling of cutting processes. *Proceedings in Manufacturing Systems*, 6(1), pp. 11-24.
- [33] Zerun Zhu, Xiaowei Tang, Chen Chen, Fangyu Peng. (2021). High precision and efficiency robotic milling of complex parts: Challenges, approaches and trends. *Chinese Journal of Aeronautics*, 35(5). DOI:10.1016/j.cja.2020.12.030.



- [34] Wei Ji, Lihui Wang. (2019). Industrial robotic machining: a review. *The International Journal of Advanced Manufacturing Technology*, 103(1-4), pp. 1239-1255. DOI:10.1007/s00170-019-03403-z.
- [35] Zhang, J., Huang, X., Kang, X., Yi, H., Wang, O., Cao, H. (2023). Energy field-assisted high-speed dry milling green machining technology for difficult-to-machine metal materials. *Frontiers in Mechanical Engineering*, 18(2), 28. DOI: 10.1007/s11465-022-0744-9.
- [36] Jiawei Wu, Xiaowei Tang, Shihao Xin, Chenyang Wang, Fangyu Peng, Rong Yan. (2024). Research on the directionality of end dynamic compliance dominated by milling robot body structure and milling vibration suppression. *Robotics and Computer-Integrated Manufacturing*, 85, 102631. DOI:10.1016/j.rcim.2023.102631.
- [37] Toni Cvitanic, Vinh Nguyen, Shreyes N. Melkote. (2020). Pose optimization in robotic machining using static and dynamic stiffness models. *Robotics and Computer-Integrated Manufacturing*, 66(4), 101992. DOI:10.1016/j.rcim.2020.101992.
- [38] Tengyu Hou, Yang Lei, Ye Ding. (2023). Pose optimization in robotic milling based on surface location error. *Journal of Manufacturing Science and Engineering*, 145(8). DOI:10.1115/1.4057055.
- [39] Yuan Xue, Zezhong Sun, Shiwei Liu, Dong Gao, Zefan Xu. (2022). Stiffness-Oriented Placement Optimization of Machining Robots for Large Component Flexible Manufacturing System. *Machines*, 10(5), 389. DOI:10.3390/machines10050389.
- [40] Rusanovskii, S. A., Khudyakov, M. P. (2021). Design of Production Systems. 3. Tool Design. *Russian Engineering Research*, 41(1), pp. 16–18. DOI: 10.3103/S1068798X21010196.